Effects of Geometric Modifications on a Complex Multi-Stream Supersonic Rectangular Nozzle

Emma D. Gist[*,a], Seth W. Kelly[*,a], Tyler M. Vartabedian[†,a], Rishov Chatterjee[‡,a], Parshwanath S. Doshi[*,b], Mark N. Glauser[§,a], Datta V. Gaitonde[§,b]

Mechanical and Aerospace Engineering

[a]Syracuse University
Syracuse, NY

[b]The Ohio State University
Columbus, OH

Experimental measurements are performed to analyze the effects of passive control on a supersonic multi-stream rectangular nozzle. The configuration explored consists of a supersonic core stream (M = 1.6) and a sonic (M = 1) bypass stream which merge behind a splitter plate exiting into a Single Expansion Ramp Nozzle (SERN) and onto an aft-deck. Previous studies have deduced that the aft-deck geometry can alter the plume deflection and farfield acoustics, while the splitter plate has an influence on the shock train development and unsteady loading on the aft-deck due to the shedding instability behind the splitter plate. This campaign seeks to exploit the inherent receptivity of these regions by performing geometric modifications as a form of passive control. The study is broken down into two separate parts, the first being the aft-deck changes. Aft-decks explored vary parameters such as length, width, and chamfer from the nominal design to observe the influence of each on the flow. Comparison to the nominal, half nominal, and no deck cases are in agreement with previous studies and show the plume deflection being a result of the shock train development. All deck modifications showed a slight upward deflection of the jet plume. The second effort of this study is the exploration of a sinusoidal spanwise wavenumber to the splitter plate trailing edge. Experimental design of the splitter plate is guided by Large Eddy Simulations (LES) performed by The Ohio State University. Particle Image Velocimetry and farfield acoustics are recorded for a wavenumber of 0.8 to match that of the LES. Both simulations and experiments show a reduction in the dominating tone. Results from both forms of passive control are compared with and used for validation of simulations.

I. Nomenclature

LES	=	Large Eddy Simulation
$SPTE$	=	Splitter Plate Trailing Edge
PIV	=	Particle Image Velocimetry
NPR	=	Nozzle Pressure Ratio
$SERN$	=	Single Expansion Ramp Nozzle
$MARS$	=	Multi-Aperture Rectangular SERN
$SBLI$	=	Shockwave Boundary Layer Interactions
D_h	=	Hydraulic Diameter
D_e	=	Effective Diameter
h_e	=	Nozzle exit height
w	=	Nozzle width
β	=	Spanwise wavenumber

[*]PhD Student
[†]MS Student
[‡]BS Student
[§]Professor, AIAA Fellow

II. Introduction

As performance requirements for engines have increased, so has the need for less conventional engine designs. One such example is the rectangular nozzle, whose complexity is outweighed by additional benefits such as thermal management [1] and enhanced stealth capabilities [2]. This study employs a modern nozzle design coupled with a variable cycle engine concept by Simmons [3] displayed in Fig. 1. The design consists of a core stream, primary bypass and secondary bypass which exit into a Single Expansion Ramp Nozzle (SERN). Addition of the secondary bypass, or third stream, has been shown to provide benefits such as decreasing noise [4–6], improving operating efficiency [3], and can shield the aft-deck from thermal loading [1].

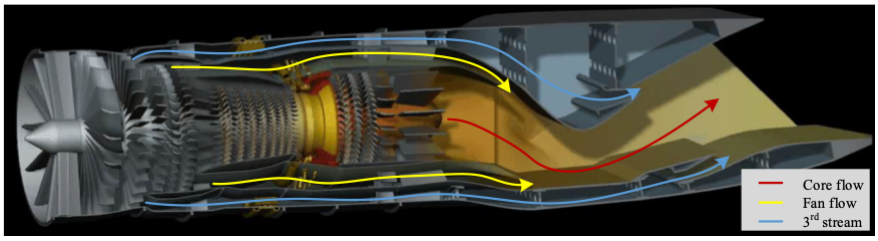

Fig. 1 Variable Cycle Engine Studied by Simmons [3].

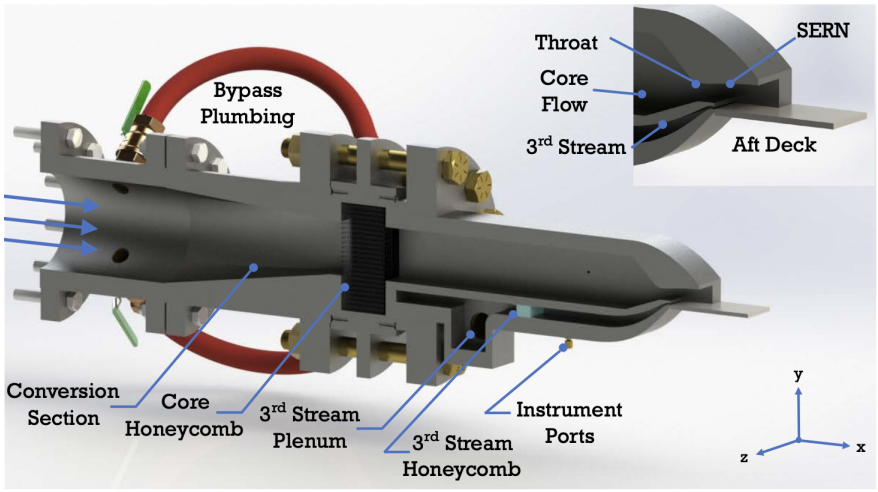

Fig. 2 Rendering of the Experimental MARS.

Experimental configuration of this design is denoted the Multi-Aperture Rectangular SERN (MARS), displayed in Fig. 2. The nozzle design assumes a premixed core and primary bypass, referred to as the first stream in this paper and secondary bypass, which will be called the third stream, that are separated by a splitter plate. Design operating conditions maintain a first stream of mach 1.6 and a third stream of mach 1 of varying densities. Both streams merge behind the splitter plate before exiting into the SERN and over the aft-deck, which essentially mimics airframe integration. The turbulent flowfield consists of a complex shock-expansion wave system, shock-wave boundary layer interactions (SBLI), various boundary layers, and shear layers. Complexity of the flowfield is established by the SERN, splitter plate, and aft-deck. Aft-deck length has been explored in detail experimentally by Berry [7–10] and Magstadt [11, 12], and using high fidelity Large Eddy Simulations (LES) by Stack & Gaitonde [13, 14] at the same flow conditions.

The aft deck has been shown experimentally to have effects on the shock train as well as the shape and deflection of the core jet plume [7]. Through LES, Stack [14] shows the plume deflection is connected to the shock train. Stack demonstrates that by adjusting the nozzle pressure ratio (NPR) and/or the deck length, the pressure field in the aft deck region is affected which subsequently affects the shock-train and resulting plume deflection. The previous studies have focused on the nominal deck length or those shorter than the nominal length with the exception of Gist *et. al* [15] that skims the surface of the effects of a deck extending past the nominal length.

Another advantageous component of the MARS is the third stream. The addition of the third stream to this design

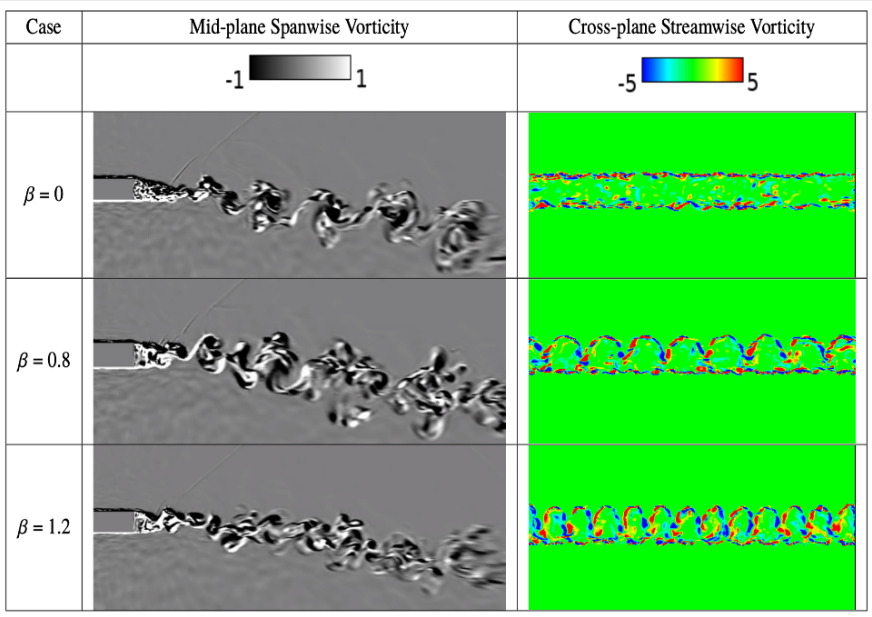

Fig. 3 Vorticity. Left: Gray scale representation of spanwise vorticity for the three cases at the centerline plane. Right: Streamwise vorticity one SPTE thickness downstream. [15]

can shield the aft-deck from the shock downstream [16] and provide a thermal barrier to the deck [1]. However, the effectiveness of the third stream has been shown by the previously mentioned studies for this nozzle to be compromised by the shedding instability in the region of the splitter plate. Impact of this instability has been shown to have global detriment both acoustically and in terms of unsteady aft-deck loading. The dominating tone in the farfield has been linked to the vortex shedding instability of the splitter plate and occurs at half of the shedding frequency, 34 kHz for design operating conditions. The frequency of the shedding is controlled by the third stream speed [11], that varies the characteristic frequency between 32-35kHz. Simulations performed by the High-Fidelity Computational Multi-Physics Laboratory at The Ohio State University [15] provide evidence that an introduction of a non-zero spanwise wavenumber can alter the SPTE instability and reduce the dominant tone. Probes were used in simulations to investigate the effect of the wavenumber on the tone. A virtual probe was placed in the primary shock, the shear layer, the core stream and the deck stream, which each showed the distinct high frequency tone for the nominal ($\beta = 0$) splitter plate case. In both non-zero beta cases, the presence of this tone was not as prominent or in some cases diminished completely. Effects of the introduced wavenumber on the flow physics can be seen in Fig. 3, where the zero beta case shows coherent spanwise vortices. As the wavenumber increases, the number of lobed pairs of positive and negative streamwise vorticity increases. The introduction of this streamwise vorticity due to the SPTE wavenumber interrupts the formation of the spanwise vortices as can be seen in spanwise vorticity plots of Fig. 3. This leads to increased mixing between the layers and reduces the appearance of coherent structures shedding behind the splitter plate.

The receptive nature of this region has been demonstrated by researches such as Ruscher *et. al* [16], who compared the nominal splitter plate to a knife-edge SPTE design for the MARS. For the knife-edge case, the SPTE was thinned and the third stream was introduced to the first stream at an angle. LES of both configurations showed the knife-edge case to have a drastic effect on the shock-train evolution. The SPTE instability in the knife-edge case becomes more shear driven, which matches the findings of Stack [14] who performed LES for various splitter plate thicknesses. In both studies, as the instability became more shear driven, the shear layer provided shielding of the aft-deck from the reflected shock downstream,proving advantageous in a loading perspective.

Demonstrated receptivity of the aft-deck and SPTE make these regions excellent candidates for flow control. Two forms of passive control are explored to the aforementioned nozzle components, both dealing with geometric modifications. The first is the modification of the aft-deck, more specifically, the length and chamfer of the trailing edge corners. In addition, geometric modifications to the SPTE are investigated. A wavenumber of $\beta = 0.8$ is used to match simulations and is compared to the nominal splitter plate case.

III. Passive Control Techniques

A. Aft-Deck Modifications

Deck plate geometries have been designed and manufactured previously by DiDominic *et. al*. [17], on the premise of minimizing the acoustics via predictive capabilities of neural networks. The following explores such aft-deck modifications with the intention of determining the consequences of these modifications on the flow physics.

Aft-Deck	Length (in)	Width (in)
Nominal	3.5625	5.2500
Twice Nominal	7.125	5.2500
Triangle	7.125	5.2500
Infinite Width	3.3125	12.1875

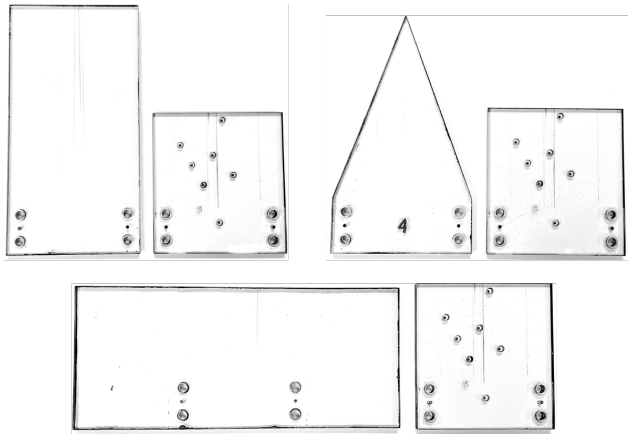

Fig. 4 Twice nominal, triangle, and infinite deck plates compared to nominal case.

Previous campaigns for flow physics at the Syracuse experimental SERN facility have focused solely on modifying the length of the aft deck; data has been acquired for the no deck, half deck, and nominal deck configurations. Of the newly designed decks, three were chosen for analysis; one deck varies length, one trailing edge chamfer, and one width (proposed by Dr. Gregg Abate [18]). These modifications, seen in Fig. 4, correspond to the assigned deck names twice nominal, triangle, and infinite width. These designs were chosen as they were the most extreme modifications of each parameter. The twice nominal length extended as far downstream as possible with insignificant deflection from the polycarbonate deck. In addition to the length modification, changes to the chamfer of the aft-deck is studied to determine the impact on the propagation of corner vortices. The most extreme chamfer case, the triangle plate, represents the situation where the corner flows emanating from the nozzle exit on the deck side are least bound by the plate itself (of the four plates shown here), allowing for the formation of corner vortices further upstream on the deck side and increased mixing between the core flow and ambient air. The last modification studied is a quasi-infinite width deck with a width of $\sim 7D_h$, extending far past the the nozzle edges. The infinite plate acts as a contrast to the triangle plate, as it is the case where the corner flows are the most bounded by the deck geometry. The plate acts as if it is infinite in the z direction functioning as a nozzle configuration fully integrated into an airframe.

This campaign seeks to explore the three variations mentioned above utilizing particle image velocimetry (PIV) and farfield pressure measurements.

B. Splitter Plate Trailing Edge Modification

An alternative SPTE design is explored to match the simulations in [15]. The smallest wavenumber, $\beta = 0.8$, non-dimensionalized by the SPTE thickness, has been deemed the most feasible from a machining aspect. Although a reduction in the SPTE thickness was shown to have a direct impact on reducing energies of turbulent instabilities [16] (most importantly the splitter plate shedding instability discussed prior), a constant thickness is followed for this study to directly focus on the impact of the introduced wavenumber. Fig. 5 displays the splitter plate that has been implemented in the MARS.

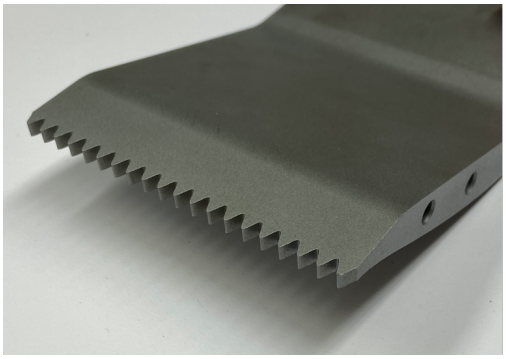

Fig. 5 Machined splitter plate with wavenumber $\beta = 0.8$.

C. Measurement Techniques

A combination of Particle Image Velocimetry (PIV) and pressure measurements are used to analyze the response to the passive control methods proposed above. PIV and farfield microphones are sampled simultaneously with a minimally heated nozzle. All experiments took place in the anechoic chamber at Skytop Turbulence Laboratory at Syracuse University.

1. Particle Image Velocimetry

PIV is used to calculate the vector fields at the nozzle exit and downstream. Stereoscopic PIV utilizes tracer particles illuminated by a pulsed laser sheet which are recorded by two cameras at varied angles in order to capture three components of velocity in a two-dimensional plane. With the lasers and cameras both mounted to a two-axis traverse, multiple tests can be run at different planes in space. These planes normal and inline to the flow are denoted the cross stream and streamwise directions respectively, shown in Fig. 6. Plane locations are normalized by the nozzle hydraulic diameter (D_h), which $D_h = 44.5\ mm$ for the MARS. To gain insight into the 3-D nature of this flowfield, streamwise measurements are taken at z/D_h = -1, 0, 0.25, 0.5, 0.75, 1. Cross stream measurements are taken at x/D_h = 4, 5, 6, 7, 8 for analyzing the evolution of the corner vortices. Each PIV run consists of 800 images acquired at a rate of 10Hz. For each plane location, 2400 images are obtained. Due to the slow rate of acquisition averaged velocities, over the 2400 statistically independent images, are compared between the different configurations.

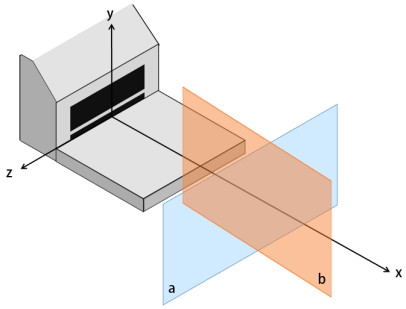

Fig. 6 Plane orientations for (a) cross stream and (b) streamwise PIV.

2. Pressure Measurements

Farfield pressure probes are used concurrently with PIV. A circular array of 10 microphones is positioned relative to the effective diameter (D_e) in the farfield approximately 85.6 D_e downstream of the nozzle in the sideline plane. The microphones are positioned in steps of 15° from 90° to 135° and increments of 5° from 135° to 165°, with 90° being perpendicular to the nozzle exit. A visualization of the microphone locations relative to the nozzle can be seen in Fig. 7. The microphones are sampled simultaneously at 100 kHz to capture high frequency content in the flow.

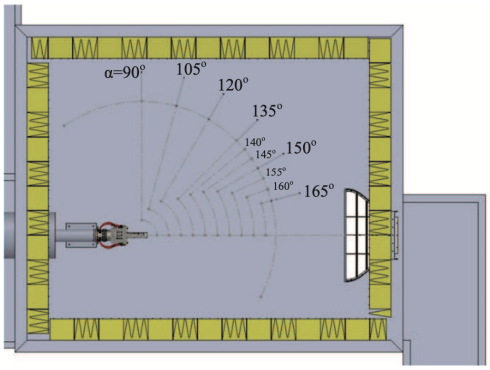

Fig. 7 Farfield microphone array in Skytop Turbulence Facility.

IV. Results

A. Aft-Deck Length Effects

Three deck plates are explored qualitatively in this section for the nominal splitter plate MARS; each of which are compared to the nominal, half and no aft-deck configurations. For the purpose of comparison, the color bars for the PIV contour plots will not be altered to potentially see the shocks more clearly but instead be held constant over all plots.

1. Streamwise PIV

The first comparison is made with the twice nominal deck and is compared with PIV in Fig. 8. Examination of the centerline plane, $z/D_h = 0$, for the various lengths provides initial evidence that the twice nominal deck most closely resembles that of the nominal deck. The twice nominal deck has the same separation region as the nominal, that begins just after the first shock impinges on the deck plate. For the nominal deck, this region ends at $x/D_h = 2$ which is the end of the deck. In the twice nominal case, there appears to be reattachment close to $x/D_h = 2$ like in the nominal case; However, since the deck continues in the x direction after this point, an additional separation region is seen from approximately $x/D_h = 2.5$ to $x/D_h = 4$. This second separation region extends slightly further in the y direction than the first did.

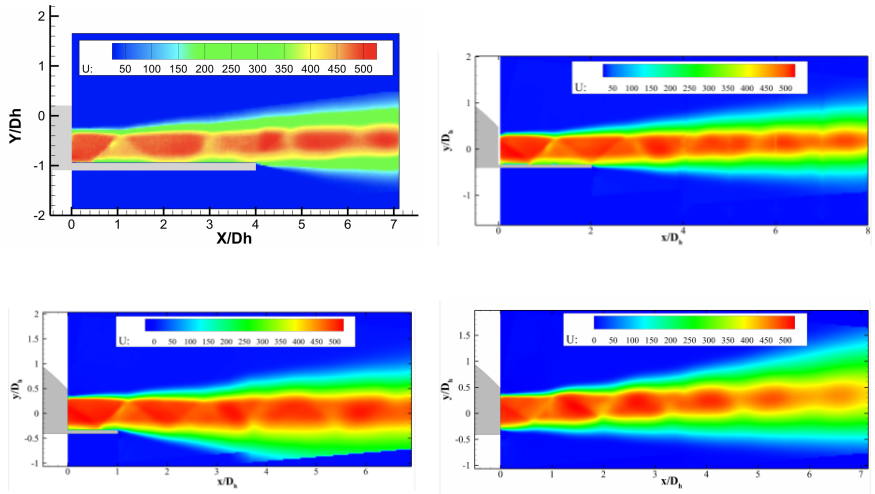

Fig. 8 Left to Right and Top to Bottom: Twice Nominal, Nominal, Half, and No deck configurations of time averaged u-component of velocity taken at z/D_h = 0.

Fig. 9 shows the infinite and triangle aft-deck centerline planes. The infinite, as expected, is very similar to the nominal deck centerline contour because the length of both decks is the same. They shock locations and speeds of both

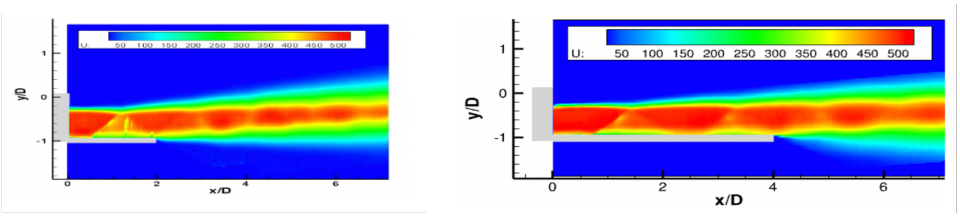

Fig. 9 Centerline streamwise u-component of velocity for the Left: infinite aft-deck. Right: triangle aft-deck.

are almost identical, including the separation region that starts in the middle of the deck and reattaches at the end of each deck. The triangle deck, which is the same length as the twice nominal also appears to have the second separation region from x/D_h = 2.5-4. All of the three aft-deck designs studied here show a slight deflection upwards in the plume after the deck. This is inline with the no deck and nominal deck configurations. The only deck showing a downward deflection of the jet plume is the half-deck design.

2. Cross stream PIV

This section explores the effect of deck geometry on the evolution of corner vortices for the nozzle with preliminary results of the nominal splitter plate. Fig. 10 shows the evolution of the infinite and twice nominal decks from x/D_h = 4-5. The flow of the infinite deck configuration is not bounded by the deck this far downstream, as the plate ends at x/D_h = 2. The twice nominal deck, on the otherhand, ends at x/D_h = 4 and is therefore displayed in the top right image of Fig. 10. Initially, the cross stream plots have a similar out of the plane velocity contour with the main difference being that the twice nominal flow is still bounded by the deck at this location. Further downstream however, there is a more distinct difference in the unbounded flowfields. The twice nominal appears less orderly than the infinite over the same number of averaged ensembles, compared to the elliptical high speed region of the infinite measurements.

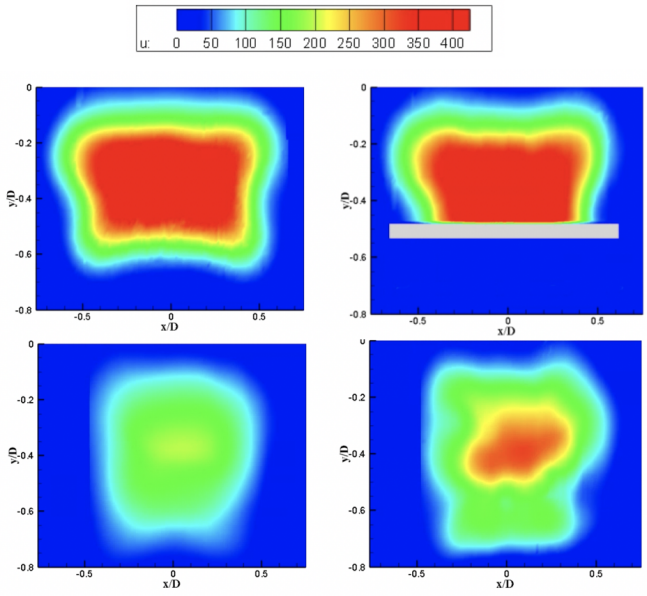

Fig. 10 Cross stream measurements for Left: Infinite Deck. Right: Twice Nominal deck. Top: x/D_h = 4. Bottom: x/D_h = 5.

B. Wavy Splitter Plate

The second form of passive control is a geometric modification to the SPTE, where a wavenumber of $\beta = 0.8$ is introduced. Preliminary results compare the centerline streamwise plane of the no deck, half deck and nominal deck for each splitter plate; the first and third streams maintained design operating conditions of Mach 1.6 and Mach 1 respectively.

1. Acoustics

Far field measurements of the nominal aft-deck, in Fig. 11, shows a clear diminishment of the high frequency tone for the 120° microphone. This finding is consistent with simulation results of the same wavenumber [15]. The 34 kHz tone in the nominal plate case was found to be diminished in the case of the wavy splitter plate. The overall sound pressure levels for each microphone are displayed in Fig. 12. OASPL for each microphone location indicates higher values for the sideline angles of the wavy splitter plate. Though the high frequency peak was reduced in the spectra, integration under the two OASPL curves provides effective sound pressures that are within one dB of each other.

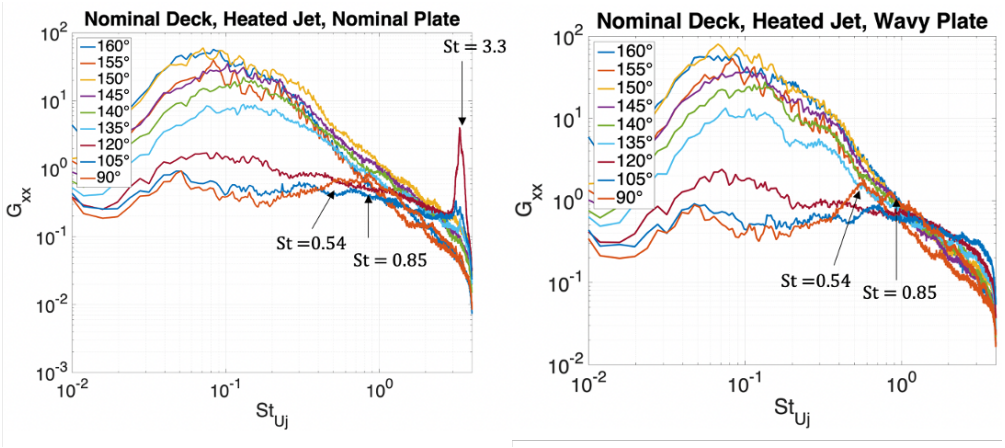

Fig. 11 Single-sided autospectral density for the nominal aft-deck configurations with the nominal and wavy splitter plates.

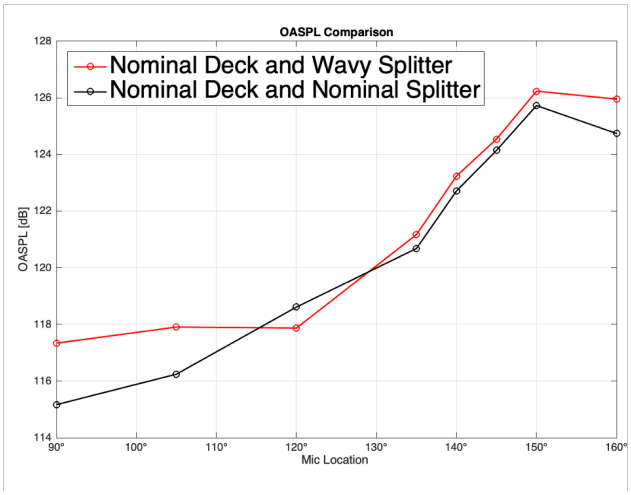

Fig. 12 Overall Sound Pressure Levels for each microphone for the nominal aft-deck with the wavy and nominal splitter plate cases.

This could be due to the increase in amplitude of the two lower Strouhal peaks. Additional inspection of the spectra shows two peaks at St = 0.54 and St = 0.85 for both splitter plates, with the amplitude being higher at both Strouhal

numbers in the case of the wavy plate. Further investigation is to be done to determine the source of these frequencies.

For the no deck configurations, the 34kHz tone is again diminished for the wavy splitter plate. The spectra has peaks at St = 0.25 and St = 0.43. The lower frequency has been attributed to screech by Berry [7]. The amplitude, however, for the screech tone is higher in the wavy splitter plate case. Additional analysis will be performed to determine why this may be.

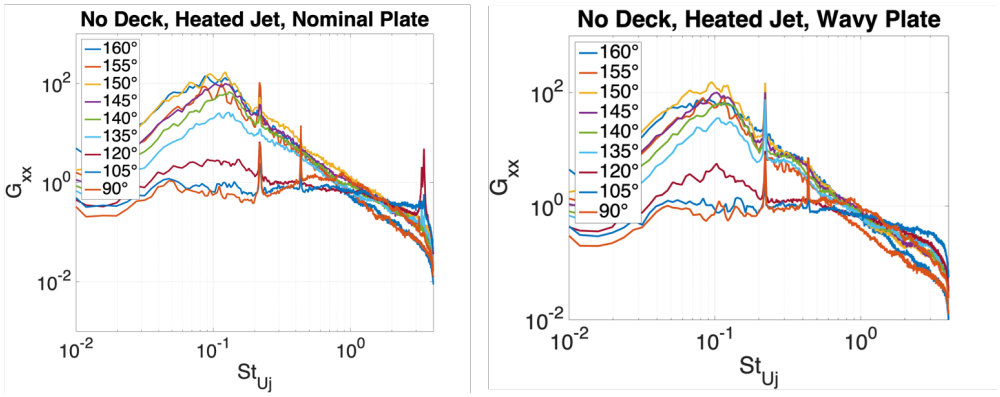

Fig. 13 Single-sided autospectral density for the no aft-deck configurations with the nominal and wavy splitter plates.

2. PIV

Preliminary PIV for the sinusoidal splitter plate is displayed for the no deck and nominal deck nozzle designs at the centerline streamwise plane. The no deck configuration, in Fig. 14 represents the least bounded case for the side with the wall jet. Here, the averaged u-component of velocity is only averaged over 1600 images instead of 2400 images due to time constraints. However, the shear layers appear to be more thick in the case of the wavy plate. The shocks appear to be in the same locations for both splitter plates but it is important to note that the colormaps were matched to that of the nominal data instead of adjusting the colormap to potentially see more distinct shocks or other features in the sinusoidal plots used in this section.

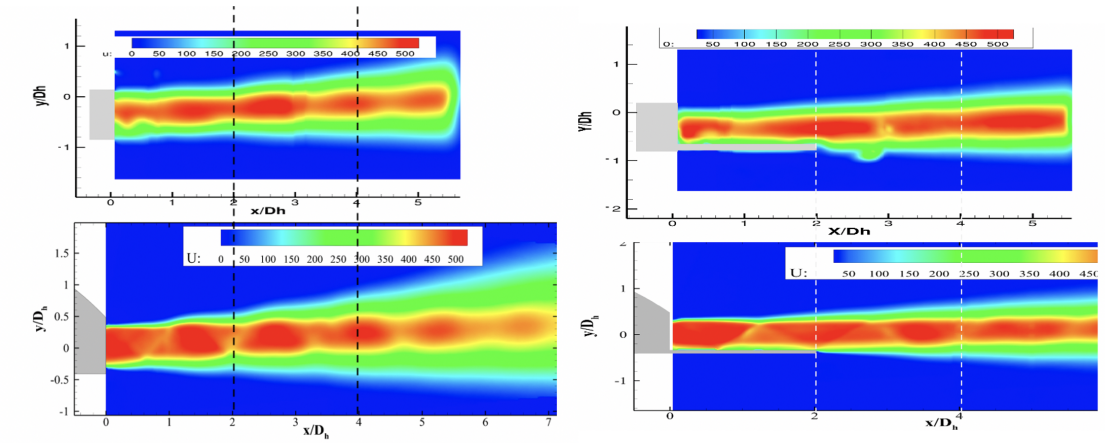

Fig. 14 Averaged u-component of velocity for z/D_h = 0 for the Left: no aft-deck. Right: Nominal aft-deck. Top: Sinusoidal SPTE. Bottom: Nominal SPTE.

Nominal aft-deck comparisons of the two splitter plates are in Fig. 14. The number of image pairs averaged over for each contour is the same however the shocks do not appear as well defined in the wavy case. The separation region on the deck appears to be longer in the wavy SPTE case. Additionally, at approximately x/D_h = 2.9, there is a stationary

feature which will be investigated further during this campaign.

V. Conclusions and Future Work

Two forms of passive control were implemented to multi-stream rectangular SERN. The first was a geometric change to the length, chamfer and width of the aft-deck plate. The streamwise centerline plane for each deck was compared. The twice nominal deck appeared to have the same separation region as the nominal, with an additional separation from $x/D_h = 2.5$ to $x/D_h = 4$. The second geometric modification to the MARS was the introduction of a wavenumber to the SPTE. The wavenumber was guided by simulations from the the High-Fidelity Computational Multi-Physics Laboratory at The Ohio State University. Simulations showed an introduction in streamwise vorticity that broke up the spanwise vortices shed from the splitter plate and diminished the dominant tone. Farfield acoustic spectra showed agreement with simulations, as the high frequency tone was not present for the wavy splitter plate in various configurations. Reduction of this tone was offset for OASPL by the increase in amplitude of lower frequency tones for the nominal aft-deck and no deck.

Additional flowfield analysis is to be performed for the sinusoidal SPTE by the continuation of the PIV planes established in Section III.C. Near field pressures will be obtained via Kulites integrated into the aft-deck and used to provide insight of the 3D nature of the flow in the near field of the nozzle.

Acknowledgments

This study was provided funding by the Air Force Office of Scientific Research (AFOSR) grant number FA9550-19-1-0081, Dr. Gregg Abate, program manager. The authors would like to thank Aleksandar Dzodic and Vincent Miczek of Skytop Turbulence Laboratory for their hard work and dedication to this project, along with the High-Fidelity Computational Multi-Physics Laboratory from The Ohio State University for providing simulations for comparison.

References

[1] Bruening, G. B., and Chang, W. S., "Cooled cooling air systems for turbine thermal management," *ASME Paper*, Vol. 14, 1999, p. V003T01A002.

[2] Katz, D., "A closer look at stealth, part 5: Nozzles and ex- hausts." 2017. https://doi.org/http://aviationweek.com/program-management-corner/closer-look-stealth-part-5-nozzles-and-exhausts#slide-0-field_images-1655211.

[3] Simmons, R. J., "Design and control of a variable geometry turbofan with and independently modulated third stream," Ph.D. thesis, The Ohio State University, 2009.

[4] Magstadt, A., Berry, M., Shea, P., Glauser, M., Ruscher, C., Gogineni, S., and Kiel, B., "Aeroacoustic experiments on supersonic multi-aperture nozzles," *53rd AIAA/ASME/SAE/ASEE Joint Propulsion Conference*, Orlando, FL, 2015.

[5] Berry, M. G., Magstadt, A. S., Glauser, M. N., Ruscher, C. J., Gogineni, S. P., and Kiel, B. V., "An acoustic investigation of a supersonic, multi-stream jet with aft deck: Characterization and acoustically-optimal operating conditions," *54th AIAA Aerospace Sciences Meeting*, 2016, p. 1883.

[6] Papamoschou, D., and Debiasi, M., "Directional suppression of noise from a high-speed jet," *AIAA journal*, Vol. 39, No. 3, 2001, pp. 380–387.

[7] Berry, M. G., "Investigating the Interaction of a Supersonic Single Expansion Ramp Nozzle and Sonic Wall Jet," Ph.D. thesis, Syracuse University, 2016.

[8] Berry, M., Magstadt, A., and Glauser, M. N., "Application of POD on time-resolved schlieren in supersonic multi-stream rectangular jets," *Physics of Fluids*, Vol. 29, No. 2, 2017, p. 020706.

[9] Berry, M. G., Stack, C. M., Magstadt, A. S., Ali, M. Y., Gaitonde, D. V., and Glauser, M. N., "Low-dimensional and data fusion techniques applied to a supersonic multistream single expansion ramp nozzle," *Physical Review Fluids*, Vol. 2, No. 10, 2017, p. 100504.

[10] Berry, M. G., Stack, C. M., Magstadt, A., Gaitonde, D., and Glauser, M., "Analysis of a rectangular supersonic multi-stream jet by LES and experiments," *Turbulence and Shear Flow Phenomena*, Vol. 10, 2017.

[11] Magstadt, A. S., "Investigating the Structures of Turbulence in a Multi-Stream, Rectangular, Supersonic Jet," Ph.D. thesis, Syracuse University, 2017.

[12] Magstadt, A. S., and Glauser, M. N., "Stereo PIV Measurements in a Multi-stream, Rectangular, Supersonic Jet," *2018 AIAA Aerospace Sciences Meeting*, 2018, p. 0054.

[13] Stack, C. M., and Gaitonde, D. V., "Shear Layer Dynamics in a Supersonic Rectangular Multistream Nozzle with an Aft-Deck," *AIAA Journal*, Vol. 56, No. 11, 2018, pp. 4348–4360.

[14] Stack, C. M., "Turbulence Mechanisms in a Supersonic Rectangular Multistream Jet with an Aft-Deck," Ph.D. thesis, The Ohio State University, 2019.

[15] Gist, E., Doshi, P., Kelly, S., Glauser, M., and Gaitonde, D., "Exploratory Passive Control Study of a Supersonic Multi-Stream Nozzle Flow," *2020 AIAA AVIATION Meeting*, 2020.

[16] Ruscher, C. J., Gogineni, S., and Ferrill, T., "Splitter Plate Edge Effects in a Supersonic Multi-stream Nozzle," *2018 Joint Propulsion Conference*, 2018, p. 4745.

[17] DiDominic, D., Gist, E., Fitzgerald, J., and Glauser, M. N., "Complex Nozzle Optimization Techniques using Machine Learning," *AIAA Scitech 2020 Forum*, 2020, p. 1866.

[18] Abate, G., "Program Officer for Aerodynamics, AFOSR," 2019.